

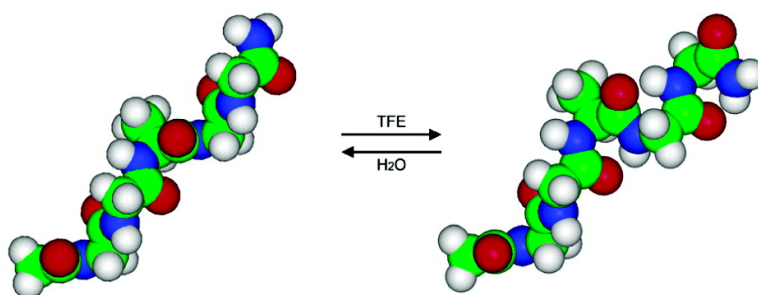
Article

Solvent Dependence of PII Conformation in Model Alanine Peptides

Zhigang Liu, Kang Chen, Angela Ng, Zhengshuang Shi, Robert W. Woody, and Neville R. Kallenbach

J. Am. Chem. Soc., **2004**, 126 (46), 15141-15150 • DOI: 10.1021/ja047594g • Publication Date (Web): 30 October 2004

Downloaded from <http://pubs.acs.org> on April 5, 2009



More About This Article

Additional resources and features associated with this article are available within the HTML version:

- Supporting Information
- Links to the 2 articles that cite this article, as of the time of this article download
- Access to high resolution figures
- Links to articles and content related to this article
- Copyright permission to reproduce figures and/or text from this article

[View the Full Text HTML](#)



ACS Publications
 High quality. High impact.

Solvent Dependence of PII Conformation in Model Alanine Peptides

Zhigang Liu,[†] Kang Chen,[†] Angela Ng,[†] Zhengshuang Shi,[‡] Robert W. Woody,[§] and Neville R. Kallenbach^{*†}

Contribution from the Department of Chemistry, New York University, New York, New York 10003, Department of Biochemistry and Biophysics, University of Pennsylvania, Philadelphia, Pennsylvania 19104, and Department of Biochemistry and Molecular Biology, Colorado State University, Fort Collins, Colorado 80523

Received April 26, 2004; E-mail: nrk1@nyu.edu

Abstract: Alanine residues in two model peptides, the pentapeptide AcGGAGGNH₂ and the 11mer AcO₂A₇O₂NH₂, have been reported to have substantial PII conformation in water. The PII structure in both peptides is sensitive to solvent. In the presence of the organic solvent TFE, the conformation of the pentamer changes from PII to internally H-bonded γ or β turns, while the chain with seven alanines forms α helix. The PII structure in the 11mer is more stable than that in the shorter peptide as the TFE concentration increases. For the pentamer, a comparison of short-chain aliphatic alcohols to water shows that the PII content decreases in the order water > methanol > ethanol > 2-propanol, linearly according to empirical scales of solvent polarity. Thus, depending on the extent of local solvation as folding progresses, the peptide backbone as modeled by alanine oligomers shifts from PII to internally H-bonded (γ or β turn) conformations and to α helix in longer segments. On the other hand, the PII content of AcO₂A₇O₂NH₂ increases significantly in the presence of guanidine, as does that of oligoproline peptides, while detergent sodium dodecyl sulfate (SDS) favors α helix in this peptide. The shorter peptide does not show a parallel increase in PII with guanidine.

Introduction

The possibility that a large class of proteins lacks stable folded structure upon extraction from the cellular milieu has focused increased attention on the nature of the conformation(s) in these molecules.¹ A complete understanding of the folding pathway of a protein requires precise definition of the unfolded state from which the reaction proceeds. Early work by Tanford's group led to a general acceptance of the view that unfolded proteins conform to polymeric random coils.² Recent SAXS data confirm that the chain dimensions of unfolded proteins scale with a power law of 0.6 consistent with coils.³ The idea that unfolded proteins conform to random or statistical coils continues to influence theory and experiments on folding, which posit that the unfolded chain has a very large conformational entropy that is overcome by accumulation of enthalpic interactions as the reaction proceeds and the native state forms.⁴ This picture leads to images of folding "funnels" that depict a progressive loss in entropy as the narrowing diameter of the funnel, while enthalpic interactions build up as the diameter shrinks. Folding emerges

in this view as an intrinsically diffusive and heterogeneous process, with a potentially large range of rates depending on how the funnel is traversed. Recent critiques have pointed out problems with this scenario.^{5–8} For one thing, folding rates tend to be simple exponentials, indicating the presence of a defined barrier. Moreover, while the overall chain dimensions of unfolded proteins are consistent with an ensemble of residues in a random coil, this proves to be a weak criterion for excluding models in which unfolded states have ordered structure.⁹ Experimentally at a finer level there are indications that significant local structure is present. Not all α helix or β structure is lost on thermal unfolding.^{10,11} Mounting spectroscopic evidence indicates that unfolded proteins contain substantial amounts of PII (poly-proline II) conformation.¹² Surveys of the conformation in unstructured regions of native proteins so-called coil libraries provide independent evidence for a significant level of PII structure in seemingly disordered subdomains.^{13,14} An

[†] New York University.

[‡] University of Pennsylvania.

[§] Colorado State University.

- (1) Baldwin, R. L. *Adv. Protein Chem.* **2002**, *62*, 361–367.
- (2) Tanford, C. *Adv. Protein Chem.* **1968**, *23*, 121–282.
- (3) Millett, I. S.; Doniach, S.; Plaxco, K. W. *Adv. Protein Chem.* **2002**, *62*, 241–262.
- (4) Eaton, W. A.; Munoz, V.; Hagen, S. J.; Jas, G. S.; Lapidus, L. J.; Henry, E. R.; Hofrichter, J. *Annu. Rev. Biophys. Biomol. Struct.* **2000**, *29*, 327–359.

- (5) Englander, S. W. *Annu. Rev. Biophys. Biomol. Struct.* **2000**, *29*, 213–238.
- (6) Plaxco, K. W.; Simons, K. T.; Ruczinski, I.; Baker, D. *Biochemistry* **2000**, *39*, 11177–11183.
- (7) Baldwin, R. L.; Rose, G. D. *Trends Biochem. Sci.* **1999**, *24*, 77–83.
- (8) Rose, G. D. *Adv. Protein Chem.* **2002**, *62*, xv–xxi.
- (9) Fitzkee, N. C.; Rose, G. D. *Proc. Natl. Acad. Sci. U.S.A.* **2004**, *101*, 12497–12502.
- (10) Shortle, D. R. *Curr. Opin. Struct. Biol.* **1996**, *6*, 24–30.
- (11) Shortle, D.; Ackerman, M. S. *Science* **2001**, *293*, 487–489.
- (12) Shi, Z.; Woody, R. W.; Kallenbach, N. R. *Adv. Protein Chem.* **2002**, *62*, 163–240.
- (13) Swindells, M. B.; MacArthur, M. W.; Thornton, J. M. *Nat. Struct. Biol.* **1995**, *2*, 596–603.
- (14) Jha, A.; Colubri, A.; Zaman, M. H.; Sosnick, T. R.; Freed, K. F. *Science*, submitted.

interesting issue then is how changes in solvation that accompany the formation of core structures in folding affect PII structure. Native proteins have nonpolar cores that exclude water, while unfolded proteins are hydrated. We address this issue here by examining the solvent-dependent conformation of short model peptides that do not acquire α helix or β strand structure under native folding conditions.

As minimal models for the unperturbed peptide backbone, alanine-containing peptides have contributed a great deal to our understanding of secondary structure formation.^{15–18} Provided that they can be prevented from intermolecular association, Ala-rich peptides of sufficient length (ca. 15–20 residues) form α helical structure at low temperature in water.^{19,20} Short chains of alanine in aqueous solution contain a significant PII population, defined as an extended conformation with dihedral angles $\phi = -75^\circ$ and $\psi = 150^\circ$. Experimental evidence comes from vibrational and NMR spectroscopic studies of blocked alanine monomers, alanyl di- and tripeptides.^{21–27} In water, longer peptides including the pentamer, AcGGAGGNH₂,²⁸ abbreviated here as G₂AG₂, in which a single alanine side chain is flanked by pairs of glycines, and an 11-mer with seven alanines flanked by pairs of basic side chains, AcO₂A₇O₂NH₂, abbreviated here as O₂A₇O₂, have NMR and CD properties corresponding to PII structure as well.²⁹ Surveys of the occurrence of PII conformation in the crystal structures of native proteins have emphasized the degree of apparent hydration surrounding residues that are in PII.^{30–33} Analysis of alanine di- or tripeptides indicates that hydration plays a key role in maintaining PII. The conformation of the blocked alanine dipeptide is found to be sensitive to nonaqueous solvents.²¹ Changing the solvent of trialanine to dimethyl sulfoxide also alters its conformation dramatically.²⁶ Extensive theoretical studies on alanine oligomers point to a role for hydration in stabilizing the backbone in PII relative to competing α or β structure.^{34–37}

The role of solvation in defining the conformational manifold in G₂AG₂ as well as the longer soluble alanine-rich peptide O₂A₇O₂ is described. We show that polar solvents, including acetonitrile, aliphatic alcohols, as well as the fluorine-substituted alcohol trifluoroethanol (TFE), alter the CD spectra of G₂AG₂. The CD spectra of G₂AG₂ in a series of simple alcohols correlate well with two empirical scales of solvent polarity, and less well with dielectric constant or any other physical property of the alcohols. This suggests a role for water itself rather than any bulk property of the solvents. In particular, TFE induces a conformation that we can assign by an NMR analysis as predominantly γ or β turn in G₂AG₂ and α helix in the case of the longer peptide O₂A₇O₂. The classical denaturing solvent GuHCl promotes PII, on the other hand. These results confirm the essential role of hydration in stabilizing PII conformation in water: depending on the solvent used, short model alanine peptides can adopt internally H-bonded turn structures, while longer chains shift to α helix.

Methods

Peptides and CD Spectroscopy. Fmoc-protected L-amino acids were purchased from NovaBiochem Corp. The O₂A₇O₂ and G₂AG₂ peptides were synthesized using a PS3 automated solid-phase peptide synthesizer (Protein Technologies, Inc.) and were purified by reversed-phase HPLC. The identities of the peptides were confirmed by MALDI mass spectrometry. CD spectra were recorded using an AVIV 202 CD spectrometer. Measurements were carried out at 1.0 nm resolution and a scan rate of 50 nm min⁻¹, averaging data from 10 scans. The instrument was calibrated with a standard made from an aqueous solution of (+)-10-camphorsulfonic acid (Aldrich, Lot KA-81867). Peptide solutions were 0.1–1.0 × 10⁻³ M, made up in spectral grade solvents. Quartz cells with path lengths of 0.1 or 1.0 cm were used for CD measurements, and spectra were recorded at room temperature, 20 °C, at wavelengths from 185 to 260 nm. The results are expressed in terms of molar residue CD.

NMR Spectroscopy. NMR spectra were acquired on a Varian Unity 500 spectrometer. The proton carrier was set at the frequency of the hydroxyl proton of TFE-d₂ (Cambridge Isotope Laboratory). Solvent signals were suppressed in all experiments using a modified WATER-GATE pulse sequence.³⁸ Proton chemical shifts were referenced to the methyl protons of the N-terminal acetyl group of G₂AG₂ at 2.05 ppm. Experimental temperatures were set to 5 °C without calibration. Proton assignments were made by the combined analysis of TOCSY and ROESY spectra.^{39,40} The Ala3 ³J_{αN} coupling constant was measured directly from the splitting of the Ala3 amide proton in 1D spectra by recording 64 k real data points. 2D ROESY data were recorded with 64 scans averaged for 2048 points collected in the T₂ dimension and 512 increments in T₁ with a spectral width of 5400 Hz in both dimensions. The ROESY mixing time was optimized at 100 ms for minimal spin diffusion effects. 2D NMR data were processed using the NmrPipe software⁴¹ and were analyzed using Sparky for ROE volume integration.⁴²

Structural Analysis. The ³J_{αN} coupling constant is related to the peptide backbone dihedral angle ϕ by a Karplus equation (eq 1).⁴³

$${}^3J_{\alpha N} = A \cos^2(\phi - 60) + B \cos(\phi - 60) + C \quad (1)$$

- (15) Marqusee, S.; Baldwin, R. L. *Proc. Natl. Acad. Sci. U.S.A.* **1987**, *84*, 8898–8902.
- (16) Scholtz, J. M.; Baldwin, R. L. *Annu. Rev. Biophys. Biomol. Struct.* **1992**, *21*, 95–118.
- (17) Rohl, C. A.; Chakrabarty, A.; Baldwin, R. L. *Protein Sci.* **1996**, *5*, 2623–2637.
- (18) Kallenbach, N. R.; Lyu, P. C.; Zhou, H. X. In *Circular Dichroism and the Conformational Analysis of Biomolecules*; Fasman, G. D., Ed.; Plenum Press: New York, 1996; pp 202–260.
- (19) Scholtz, J. M.; Qian, H.; York, E. J.; Stewart, J. M.; Baldwin, R. L. *Biopolymers* **1991**, *31*, 1463–1470.
- (20) Spek, E. J.; Olson, C. A.; Shi, Z.; Kallenbach, N. R. *J. Am. Chem. Soc.* **1999**, *121*, 5571–5572.
- (21) Madison, V.; Kopple, K. D. *J. Am. Chem. Soc.* **1980**, *102*, 4855–4863.
- (22) Han, W. G.; Jalkanen, K. J.; Elstner, M.; Suhai, S. *J. Phys. Chem. B* **1998**, *102*, 2587–2602.
- (23) Poon, C. D.; Samulski, E. T.; Weise, C. F.; Weisshaar, J. C. *J. Am. Chem. Soc.* **2000**, *122*, 5642–5643.
- (24) Woutersen, S.; Mu, Y.; Stock, G.; Hamm, P. *Proc. Natl. Acad. Sci. U.S.A.* **2001**, *98*, 11254–11258.
- (25) Eker, F.; Cao, X.; Nafie, L.; Schweitzer-Stenner, R. *J. Am. Chem. Soc.* **2002**, *124*, 14330–14341.
- (26) Eker, F.; Cao, X.; Nafie, L.; Huang, Q.; Schweitzer-Stenner, R. *J. Phys. Chem. B* **2003**, *107*, 358–365.
- (27) Weise, C. F.; Weisshaar, J. C. *J. Phys. Chem. B* **2003**, *107*, 3265–3277.
- (28) Ding, L.; Chen, K.; Santini, P. A.; Shi, Z.; Kallenbach, N. R. *J. Am. Chem. Soc.* **2003**, *125*, 8092–8093.
- (29) Shi, Z.; Olson, C. A.; Rose, G. D.; Baldwin, R. L.; Kallenbach, N. R. *Proc. Natl. Acad. Sci. U.S.A.* **2002**, *99*, 9190–9195.
- (30) Adzhubei, A. A.; Sternberg, M. J. *J. Mol. Biol.* **1993**, *229*, 472–493.
- (31) Adzhubei, A. A.; Sternberg, M. J. *Protein Sci.* **1994**, *3*, 2395–2410.
- (32) Creamer, T. P. *Proteins* **1998**, *33*, 218–226.
- (33) Stapley, B. J.; Creamer, T. P. *Protein Sci.* **1999**, *8*, 587–595.
- (34) Sreerama, N.; Woody, R. W. *Proteins* **1999**, *36*, 400–406.
- (35) Pappu, R. V.; Rose, G. D. *Protein Sci.* **2002**, *11*, 2437–2455.
- (36) Takekiyo, T.; Imai, T.; Kato, M.; Taniguchi, Y. *Biopolymers* **2004**, *73*, 283–290.
- (37) Garcia, A. E. *Polymer* **2004**, *45*, 669–676.

- (38) Pitto, M.; Sandek, V.; Sklenar, V. A. *J. Biomol. NMR* **1992**, *2*, 611–665.
- (39) Bax, A.; Davis, D. G. *J. Magn. Reson.* **1985**, *65*, 355–360.
- (40) Bothner-by, A. A.; Stephens, R. L.; Lee, J. M.; Warren, C. D.; Jeanloz, R. W. *J. Am. Chem. Soc.* **1984**, *106*, 811–813.
- (41) Delaglio, F.; Grzesiek, S.; Vuister, G. W.; Zhu, G.; Pfeifer, J.; Bax, A. *J. Biomol. NMR* **1995**, *6*, 277–293.
- (42) Goddard, T. D.; Kneller, D. G. *SPARKY 3*; University of California, San Francisco, 2003.

The most recent parameters for this equation have values $A = 7.90$, $B = -1.05$, and $C = 0.65$.⁴⁴

The rotating frame NOE, the ROE, is the dipolar relaxation effect in the transverse plane monitored while a spin lock is applied.⁴⁰ The ROE intensity between a pair of protons is proportional to the inverse sixth power of the interpair distance, as is the NOE (eq 2).

$$ROE_{vol} = A \times r^{-6} \quad (2)$$

The coefficient A for the ROE volume is a function of molecular correlation time and should be constant provided that the solute protons share a uniform relaxation rate and solvent exchange rate without considering the spin lock offset effect,⁴⁵ which applies to a small molecule such as G_2AG_2 . Protons in the peptide G_2AG_2 fall into two groups. Nonexchanging protons attached to α and β carbons scale with the peptide concentration. The ROE coefficient of carbon protons is denoted by Acc . On the other hand, amide protons are exchangeable with the solvent TFE hydroxyl proton or water, and thus less represented in the population. The ROEs between amide protons can be described by a single coefficient Ann if amide proton exchange rates are assumed to be the same for each of the five residues. The C-terminal amide protons are excluded because of their chemical self-exchange and higher solvent exchanging rate, which make the observed ROE volumes unreliable. The ROE coefficient Acn between carbon proton and amide proton is then given by eq 3⁴⁶

$$Acn = \sqrt{Acc \times Ann} \quad (3)$$

Prediction of CD Spectra. Calculation of the CD spectrum requires generation of the rotational strengths for the electronic transitions of the amide groups in the peptide. We consider three transitions in each amide: the $n\pi^*$ transition at 220 nm, the first $\pi\pi^*$ transition (NV_1) at 190 nm, and the second $\pi\pi^*$ transition (NV_2) at 139 nm. The calculation of $3N$ rotational strengths (N is the number of amide groups) proceeds in two steps. First, we use the matrix method introduced by Bayley et al. to calculate the mixing of the $3N$ transitions among themselves.⁴⁷ Such calculations have been performed for many peptides and proteins and have been reviewed recently.^{48,49} The parameters used in the present calculation are those used by Woody and Sreerama,⁵⁰ except for the direction of the NV_1 transition dipole moment, which was taken to be at -40° relative to the carbonyl bond direction, where the negative sign indicates rotation away from the CN bond direction. This differs from the direction used for proteins and for the α helix (-55°),^{50,51} based upon the results of Clark for a secondary amide.⁵² However, it is close to the experimental value for primary amides and that obtained in ab initio calculations for secondary amides.^{52–55} The less negative value was used for two reasons. (1) Calculations on the poly (Pro) II conformation give poor agreement with experiment if $\theta_{NV_1} = -55^\circ$ is used, but good agreement for -40° . (2) Calculations for the type II β turn give a positive $n\pi^*$ rotational strength for $\theta_{NV_1} = -55^\circ$, in contrast

to the negative $n\pi^*$ rotational strength obtained with $\theta_{NV_1} = -40^\circ$, the latter of which agrees with experiment.⁵⁶ It appears that $\theta_{NV_1} = -55^\circ$ is most suitable for the α -helix and β -sheets, with strong interamide hydrogen bonds, but $\theta = -40^\circ$ is preferable for the more open conformations of PPII and turns. Qualitatively, the choice of θ_{NV_1} has little effect on the predicted CD for the γ and β turn conformations, other than type II turns.

The matrix method generates the transition energies as the eigenvalues of the perturbation matrix and the excited-state wave functions as the eigenvectors. The wave function for excited-state K ($K = 1, \dots, 3N$) is:

$$\Psi_K = \sum C_{iaK} \psi_{ia} \quad (4)$$

Here, ψ_{ia} is the wave function for the peptide in which group i is in excited state a , and all other groups are in their ground state. The coefficient C_{iaK} is the element of the K th eigenvector corresponding to ψ_{ia} , and its square specifies the extent to which ψ_{ia} contributes to the eigenvector. The rotational strength of the transition to excited-state K is:⁴⁷

$$R_K \approx \text{Im}\{\mu_{0K} \cdot \mathbf{m}_{K0}\} = \sum_i \sum_a \sum_j \sum_b C_{iaK} C_{jbK} \{ \text{Im}(\mu_{i0a} \cdot \mathbf{m}_{j0b}) + (\pi/\lambda_K)(\mathbf{R}_j \cdot \mu_{j0b} \times \mu_{i0a}) \} \quad (5)$$

where μ_{0K} and \mathbf{m}_{K0} are, respectively, the electric and magnetic dipole transition moments for the transition from the ground state to excited-state K of the peptide; μ_{i0a} is the electric dipole transition moment for the locally excited state a in group i ; \mathbf{m}_{j0b} is the magnetic dipole transition moment for the locally excited state b in group j , relative to the local origin in group j ; \mathbf{R}_j is the vector from the origin of the overall peptide coordinate system to the local origin of group j ; λ_K is the wavelength of the transition to excited-state K . The summations are over all N groups and all three locally excited states.

In the second stage of the calculations, the excited states described in eq 4 are perturbed by mixing with high-energy transitions in the peptide backbone and in the side chains. Tinoco showed that the mixing of discrete transitions with the ensemble of high-energy transitions can be calculated, given polarizability tensors for bonds or other groupings.⁵⁷ Such mixing was considered in earlier calculations on the α -helix and β -sheet,^{58,59} but subsequent studies have generally neglected these contributions because of the uncertainties in the empirically derived polarizability tensors. Recently, it has proven possible to derive reliable polarizability tensors by ab initio methods. Using localized ab initio molecular orbitals, Garmer and Stevens obtained polarizability tensors for individual bonds and lone pairs that are ideally suited to calculation of the contribution of high-energy transitions to rotational strengths.⁶⁰

Using the polarizability approximation, the contribution of the high-energy transitions to the rotational strength of the transition $0 \rightarrow K$ is:

$$R_{K\alpha} = f(\lambda_K) \sum_i \sum_a \sum_j \sum_b \sum_{l \neq j} \sum_t C_{iaK} C_{jbK} \{ q_{jbt} \mathbf{R}_{jbt,l} \cdot \alpha_l \mu_{ia} \times \mathbf{R}_{it} / |\mathbf{R}_{jbt,l}|^3 \} \quad (6)$$

where $f(\lambda_K) = \pi \lambda_K / (\lambda_K^2 - \lambda_0^2)$ and λ_0 is the average wavelength of the high-energy transitions, taken to be 100 nm; q_{jbt} is a point charge located at the position \mathbf{R}_{jbt} such that $\sum_t q_{jbt} \mathbf{R}_{jbt} = \mu_{j0b}$, that is, in a monopole or distributed dipole representation of the electric dipole transition moment μ_{j0b} ; $\mathbf{R}_{jbt,l} = \mathbf{R}_j - \mathbf{R}_{jbt}$ is the vector from monopole t of transition $0 \rightarrow b$ on group j to polarizable group l , and $|\mathbf{R}_{jbt,l}|$ is the length of this vector; α_l is the polarizability tensor of group l ; and $\mathbf{R}_{it} = \mathbf{R}_i - \mathbf{R}_t$ is

(43) Schmidt, J. M.; Blumel, M.; Lohr, F.; Rüterjans, H. *J. Biomol. NMR* **1999**, *14*, 1–12.

(44) Karplus, M. *J. Chem. Phys.* **1959**, *30*, 11–15.

(45) Bax, A.; Davis, D. G. *J. Magn. Reson.* **1985**, *63*, 207–360.

(46) Nilges, M.; Macias, M. J.; O'donoghue, S. I.; Oschkinat, H. *J. Mol. Biol.* **1997**, *269*, 408–422.

(47) Bayley, P. M.; Nielsen, E. B.; Schellman, J. A. *J. Phys. Chem.* **1969**, *73*, 228–243.

(48) Hirst, J. D.; Colella, K.; Gilbert, A. T. *J. Phys. Chem. B* **2003**, *107*, 11813–11819.

(49) Sreerama, N.; Woody, R. W. *Methods Enzymol.* **2004**, *383*, 318–351.

(50) Woody, R. W.; Sreerama, N. *J. Chem. Phys.* **1999**, *111*, 2844–2845.

(51) Chin, D.-H.; Woody, R. W.; Rohl, C. A.; Baldwin, R. A. *Proc. Natl. Acad. Sci. U.S.A.* **2002**, *99*, 15416–15421.

(52) Clark, L. B. *J. Am. Chem. Soc.* **1995**, *117*, 7974–7986.

(53) Peterson, D. L.; Simpson, W. T. *J. Am. Chem. Soc.* **1957**, *79*, 2375–2382.

(54) Serrano-Andrés, L.; Fülischer, M. P. *J. Am. Chem. Soc.* **1996**, *118*, 12190–12199.

(55) Hirst, J. D.; Hirst, D. M.; Brooks, C. L. *J. Phys. Chem. A* **1997**, *101*, 4821–4827.

(56) Smith, J. A.; Pease, L. G. *Crit. Rev. Biochem.* **1980**, *8*, 315–399.

(57) Tinoco, I., Jr. *Adv. Chem. Phys.* **1962**, *4*, 113–160.

(58) Woody, R. W.; Tinoco, I., Jr. *J. Chem. Phys.* **1967**, *46*, 4927–4945.

(59) Zubkov, V. A.; Vol'kenshtein, M. V. *Mol. Biol. (Engl. transl. of Molekul. Biol.)* **1970**, *4*, 598–606.

(60) Garmer, D. R.; Stevens, W. J. *J. Phys. Chem.* **1989**, *93*, 8263–8270.

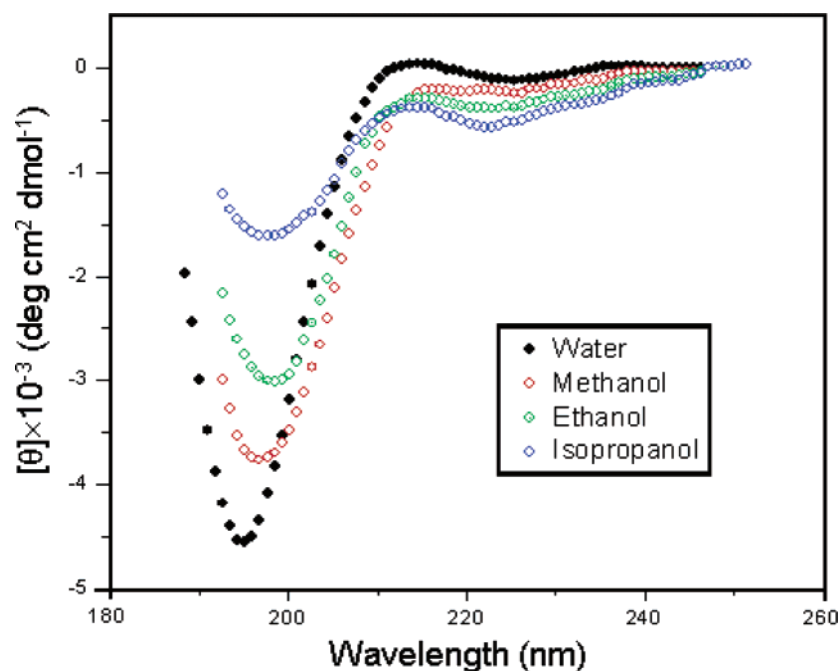


Figure 1. Far UV CD spectra of AcGGAGGNH₂ recorded in water and some neat alcohols. Measurements were carried out as described in the Methods section, at room temperature.

the vector from group i to polarizable group l . Further details of the method, the polarizability parameters, and the application to peptides in the PII conformation will be described in a subsequent publication.⁶¹

CD spectra are calculated from the theoretical wavelengths λ_K and the rotational strengths R_K , including both types of contributions, assuming Gaussian band shapes:

$$[\theta](\lambda) = 7516 \sum_K (R_K \lambda_K / \Delta_K) \exp[-(\lambda - \lambda_K)^2 / \Delta_K^2] \quad (7)$$

The parameter Δ_K is the bandwidth for the transition $0 \rightarrow K$, calculated as the weighted average of the bandwidths for the monomer transitions, Δ_{ia} :

$$\Delta_K = \sum_i \sum_a C_{iak}^2 \Delta_{ia} \quad (8)$$

These bandwidths were taken to be 10.5, 11.3, and 7.2 nm, respectively, for the $n\pi^*$, NV_1 , and NV_2 transitions.⁵⁰

The turn conformations studied were generated by the matrix methods of Ooi et al. and McGuire et al.,^{62,63} using a standard peptide geometry, standard C–C and C–H bond lengths, and tetrahedral bond angles at the α -carbon. The conformation at the C α of Ala in the γ turn conformation was assumed to be $(\phi, \psi) = (-78^\circ, +65^\circ)$, in the center of the range for the inverse γ turn.⁶⁴ The conformations of the β turns were based on the study of Venkatachalam,⁶⁵ who reported 15 conformations of three linked peptide groups that are sterically allowed and have a $4 \rightarrow 1$ hydrogen bond, with (ϕ, ψ) restricted to 30° intervals. Venkatachalam's conformation 14 corresponds to a canonical type II turn. Calculations were also performed for (1) conformations with (ϕ, ψ) closer to the (ϕ, ψ) values for γ turn, that is, Venkatachalam's conformations 8 and 10, in which the first C α of the turn has $(\phi, \psi) = (-60, +90^\circ)$ versus $(-60, +120^\circ)$ for the type II turn; and (2) modified conformations 8 and 10 in which Venkatachalam's conformation at

the first C α was converted to $(-78^\circ, +65^\circ)$, retaining the original conformations at the second C α .

The PII conformation used was $(\phi, \psi) = (-60^\circ, 170^\circ)$. This conformation differs somewhat from the canonical PII $(-77^\circ, 146^\circ)$, but is in the PII region of the Ramachandran map. Earlier studies^{66,67} have shown that the canonical PII conformation is predicted to have a strong positive couplet in the NV_1 region but that a less negative ϕ and more positive ψ yields a smaller positive couplet or even a negative couplet. Only under these circumstances is it possible to reproduce the strong negative NV_1 band observed for the PII conformation, even when high-energy transitions are included.⁶⁸ For γ turn, the two peptide groups flanking the C α of Ala were included in the calculation as well as the C α and its alkyl substituents. The CD calculated for this diamide was divided by five to calculate the ellipticity of the G₂AG₂ pentapeptide in the γ turn conformation per residue. The β turn calculations considered three peptide groups and the alkyl groups of the two C α atoms linking them. The molar ellipticity of this triamide was then divided by five to calculate the residue ellipticity of the pentapeptide.

Results

Unlike charged models, the peptide G₂AG₂ is soluble in a number of organic solvents that are sufficiently transparent to UV to allow CD measurements. Figure 1 compares far UV CD spectra of G₂AG₂ in water and a series of simple alcohols, from methanol to 2-propanol. We examined the correlation between CD signal amplitude and different physical parameters of the non-fluorine substituted alcohols, such as viscosity, dielectric constant, dipole moment, and solvent polarity. Changes in the spectral amplitude vary linearly with changes in the polarity of the solvent as expressed by empirical scales such as E_T^N and P' . E_T^N is based on the solvatochromic response of a standard dye, while P' is derived from the partition coefficients of standard substances between the vapor phase and different

(61) Woody, R. W., to be submitted.

(62) Ooi, T.; Scott, R. A.; Vanderkooi, G.; Scheraga, H. A. *J. Chem Phys.* **1967**, *46*, 4410–4426.

(63) McGuire, R. F.; Vanderkooi, G.; Momany, F. A.; Ingwall, R. T.; Crippen, G. M.; Lotan, N.; Tuttle, R. W.; Kashuba, K.I.; Scheraga, H. A. *Macromolecules* **1971**, *4*, 112–124.

(64) Rose, G. D.; Gierasch, L. M.; Smith, J. A. *Adv. Protein Chem.* **1985**, *1*–109.

(65) Venkatachalam, C. M. *Biopolymers* **1968**, *6*, 1425–1436.

(66) Madison, V.; Schellman, J. *Biopolymers* **1972**, *11*, 1041–1076.

(67) Tterlikkis, L.; Loxsom, F. M.; Rhodes, W. *Biopolymers* **1973**, *12*, 675–684.

(68) Woody, R. W. *Biophys. J.* **2004**, *86*, 617a.

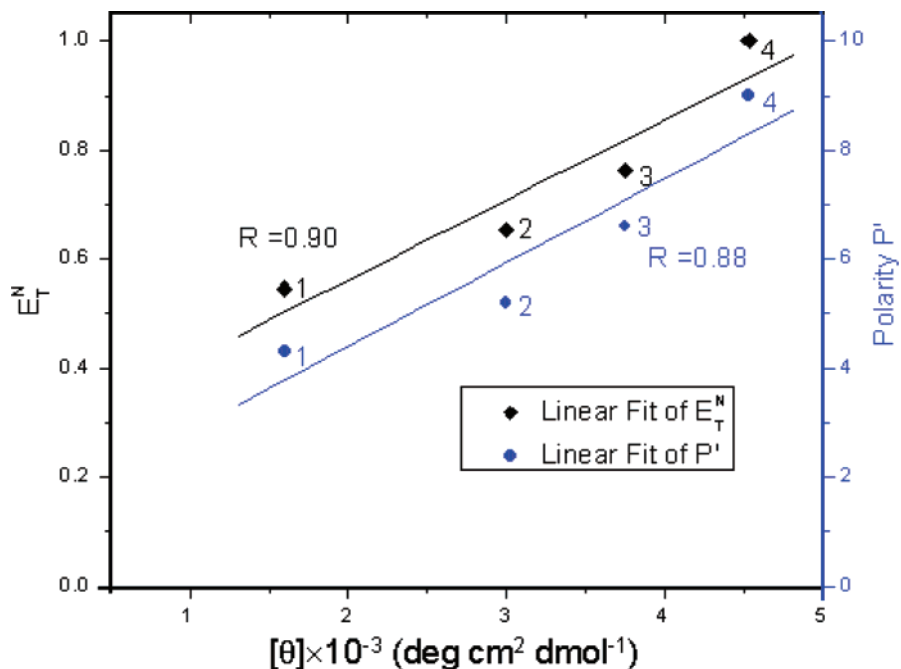


Figure 2. Correlations between CD signal (absolute value of the minimum CD signal of the peaks) of AcGGAGGNH₂ and measures of solvent polarity. Subscripts, 1–4, denote 2-propanol, ethanol, methanol, and water, respectively. The black line shows a linear fit to the E_T^N scale, and the blue one corresponds to the P' scale. The correlation coefficients are 0.90 (E_T^N) and 0.88 (P'). Both TFE and MeCN deviate strongly from the linear correlations for aliphatic alcohols.

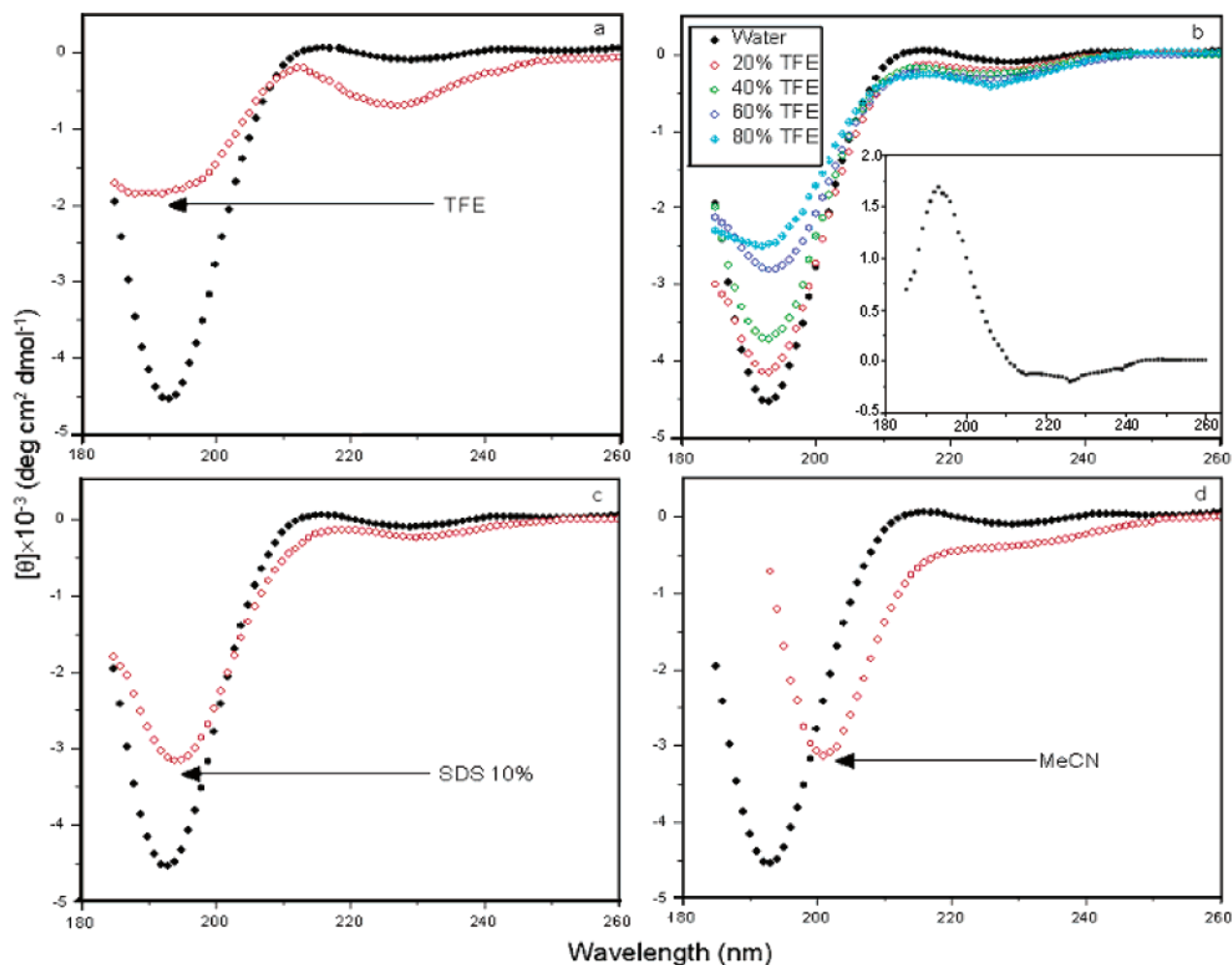


Figure 3. CD spectra of AcGGAGGNH₂ in different solvent systems: (a) TFE; (b) TFE titration, the inset spectrum is obtained by subtracting the spectrum of G₂AG₂ at 20% TFE from that at 80%; (c) 10% SDS (w/v); (d) MeCN. A spectrum of AcGGAGGNH₂ in water is shown in each panel for comparison.

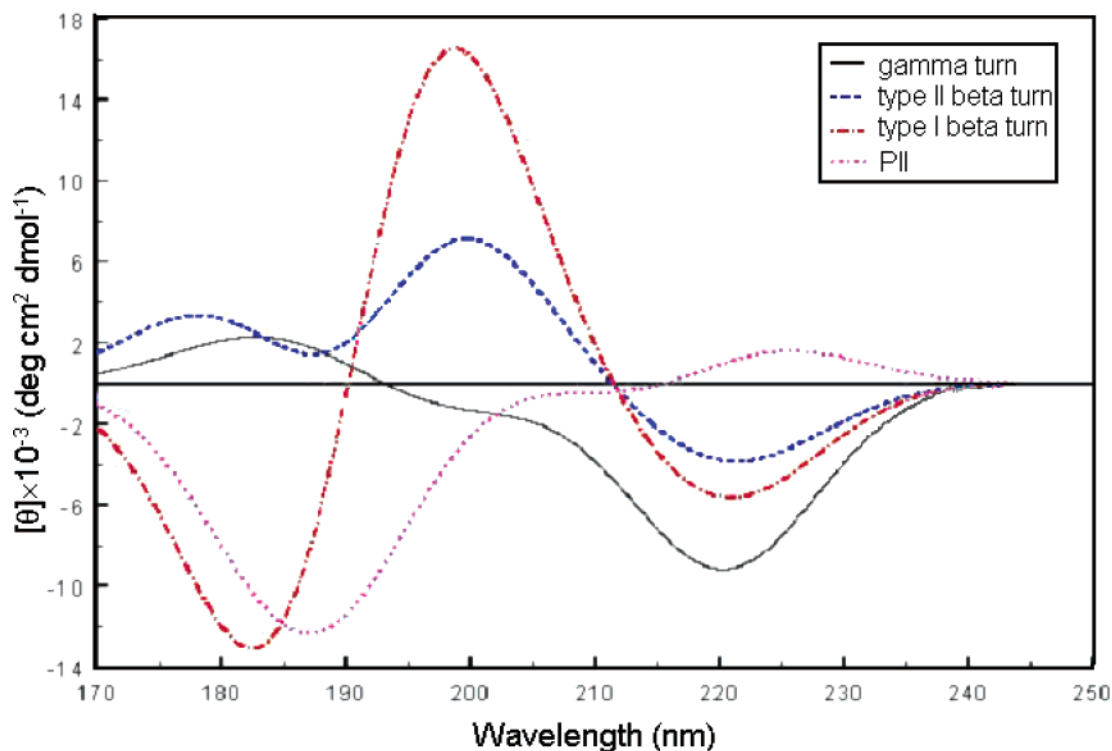


Figure 4. Calculated CD spectra of AcGGAGGNH₂ in γ and β turn conformations. PII (ϕ, ψ) = (-60° , $+170^\circ$), γ turn canonical (ϕ, ψ) = (-78° , $+65^\circ$), type I β turn canonical (ϕ, ψ) = (-60° , -30°), and type II β turn canonical (ϕ, ψ) used in this paper are from Venkatachalam's conformations 8 and 10, in which the first C α of the turn has (ϕ, ψ) = (-60° , $+90^\circ$) versus (-60° , $+120^\circ$).

solvents.^{69,70} Correlations are shown in Figure 2, and the correlation coefficients are 0.90 (E_T^N) and 0.88 (P'), respectively. The correlation with the empirical solvation scales is much better than that with the dielectric constant or any single physical property of the solvents. We believe this is important: the interactions responsible for PII stabilization reflect local solvation rather than bulk solvent properties.

Figure 3 illustrates the effects of several different solvents on the CD spectrum of G₂AG₂. Panel A shows the effect of the fluorinated alcohol TFE. A TFE titration experiment on G₂AG₂ is shown in panel B. The inset in panel B is obtained by subtracting the spectrum of G₂AG₂ at 20% TFE from that at 80%. Panel C shows the effect of 10% SDS (w/v) on the CD spectrum of G₂AG₂, while the effect of neat acetonitrile is shown in panel D. In contrast to the behavior of the aliphatic alcohols, the effects of TFE and acetonitrile do not correlate with either the E_T^N or P' scale. The anomalous solvent properties of TFE have been attributed to the formation of clusters.⁷¹

The predicted spectrum of the PII conformation has the expected features of a weak positive $n\pi^*$ band near 220 nm and a strong negative band at shorter wavelengths. The negative band is blue-shifted about 10 nm relative to the observed band for PII peptides, between 195 and 200 nm. However, this calculated spectrum reproduces the main CD features of the PII conformation far better than previous results using the matrix method.^{66,67,72} The calculated CD spectra for the γ turn and type II β turn conformations in Figure 4 show a significant negative $n\pi^*$ band near 220 nm, with the γ turn conformation more than

twice as intense as the type II β turn. The strong negative $n\pi^*$ band is a characteristic of the γ turn conformation, persisting in the calculated spectra of the β turns with a γ turn or a γ turn-like conformation at the first C α (data not shown). The predicted amplitude for the γ turn ($[\theta]_{220} \approx -9500$ deg cm² dmol⁻¹), when multiplied by five to convert to the CD per γ turn residue, is in good agreement with the experimental data of Madison and Kopple.²¹ They reported $n\pi^*$ ellipticities of $-50\,000$ for AcProNHMe and $20\,000$ for AcAlaNHMe in CHCl₃, for which NMR indicated a significant γ turn population. In the $\pi\pi^*$ region, the γ turn shows a negative shoulder at 205 nm and a positive band near 185 nm. The type II β turn has positive bands near 198 and 178 nm.

The CD spectrum of G₂AG₂ in water is consistent with a PII conformation at the Ala residue. The ellipticity per residue of ~ -5000 deg cm² dmol⁻¹ is compatible with a single residue in the PII conformation and suggests that the PII conformation at the Ala does not propagate into the GG sequences on either side. The spectra in methanol and acetonitrile are comparable in magnitude to that in water, with a red shift of ~ 5 nm. The CD spectra of G₂AG₂ in higher alcohols (ethanol and 2-propanol) have a markedly lower amplitude for the negative band near 200 nm. The very weak CD in these alcohols suggests the presence of additional conformers, in contrast to the situation in water, MeOH, or MeCN.

In TFE, the CD spectrum of G₂AG₂ has a negative band of intermediate amplitude near 200 nm and a distinct negative band near 225 nm. Madison and Kopple reported that AcAlaNHMe has $[\theta]_{200} \approx -20\,000$ deg cm² dmol⁻¹.²¹ There is strong evidence that this blocked Ala derivative has a conformation that is predominantly PII, so if the two peptide units flanking the C α of Ala in G₂AG₂ were in the PII conformation with the

(69) Reichardt, C. *Chem. Rev.* **1994**, *94*, 2319–2358.

(70) Snyder, L. R. *J. Chromatogr. Sci.* **1978**, *16*, 223–34.

(71) Hong, D.; Hoshino, M.; Kuboi, R.; Goto, Y. *J. Am. Chem. Soc.* **1999**, *121*, 8427–8433.

(72) Manning, M. C.; Woody, R. W. *Biopolymers* **1991**, *31*, 569–586.

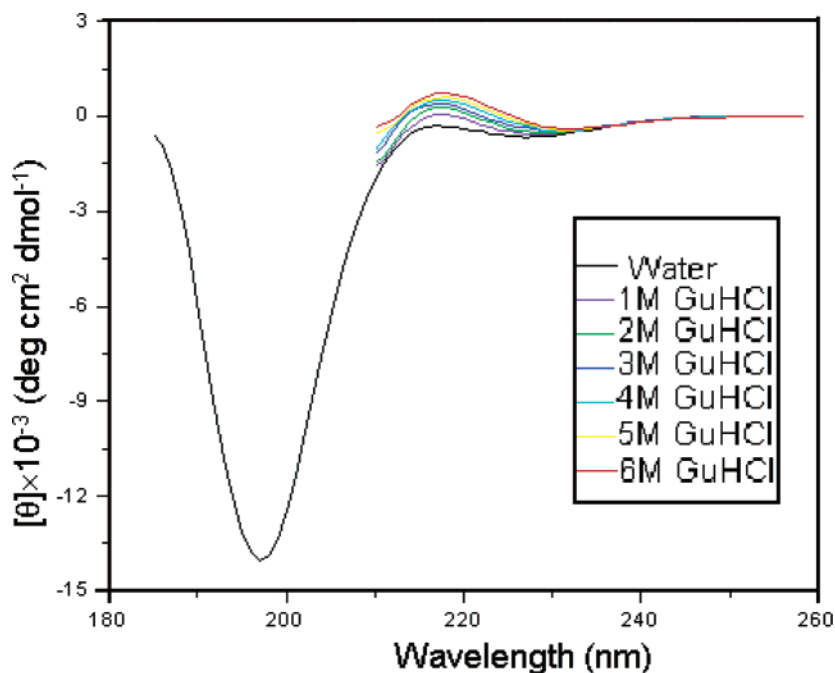


Figure 5. Effect of different concentrations of GuHCl on the CD spectrum of $O_2A_7O_2$ in the accessible range of wavelengths from 210 to 260 nm.

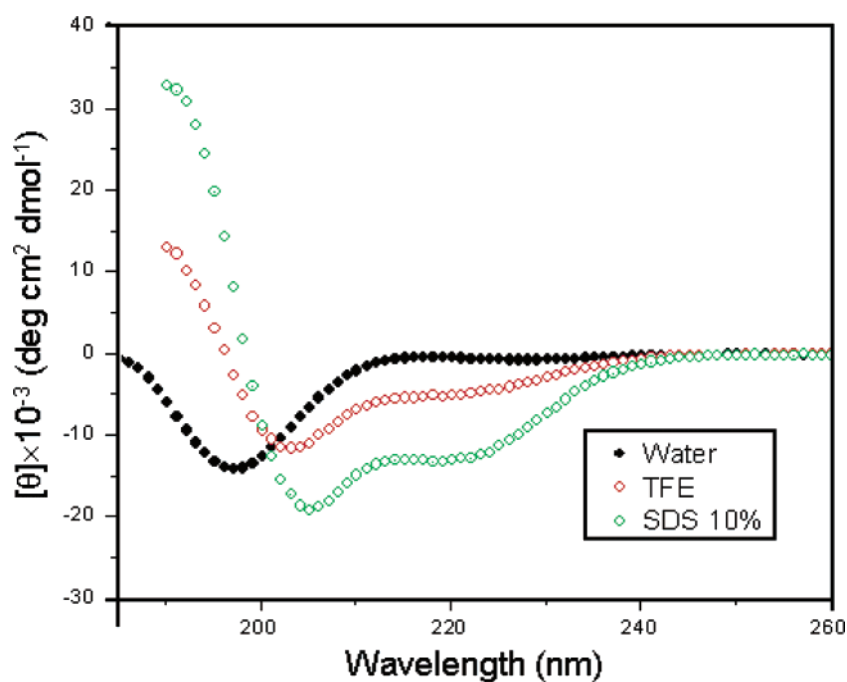


Figure 6. CD spectra of $O_2A_7O_2$ in water (20 mM NaH_2PO_4 buffer, pH 7.0.), TFE and, 10% SDS (w/v) showing an isodichroic point at 203 nm.

remaining peptide groups making negligible contributions, the 200 nm residue ellipticity of G_2AG_2 would be predicted to be $-20\,000/5 = -4000 \text{ deg cm}^2 \text{ dmol}^{-1}$. Thus, retention of the negative 200-nm band indicates the presence of the PII conformation, but its lower amplitude implies that other conformers are present. The most likely candidates are γ turn, predicted to have a weak negative CD band near 200 nm, and β turns of types I and II, which both have strong positive CD bands near 200 nm. These three conformations also have negative CD near 225 nm. Of these conformers, the γ turn conformation is compatible with the ROESY intensities, while the type I and type II β turns each have short interproton

distances that are inconsistent with the distances inferred from the ROESY intensities. Still, the quantitative CD intensities are difficult to reconcile with a two-component mixture. The weak $\pi\pi^*$ CD of the γ turn and the approximately 2-fold decrease in intensity of the 200-nm band in TFE relative to water suggests roughly equal amounts of γ turn and PII in TFE. Such a mixture should have a 225-nm ellipticity of $\sim -5000 \text{ deg cm}^2 \text{ dmol}^{-1}$, considerably larger than the observed value ($\sim -800 \text{ deg cm}^2 \text{ dmol}^{-1}$). Thus, the conformational blend is likely to be more complex; for example, TFE/water mixtures show distinct deviations from an isoelliptic point (Figure 3b), implying at least three spectroscopically significant conformers. The difference

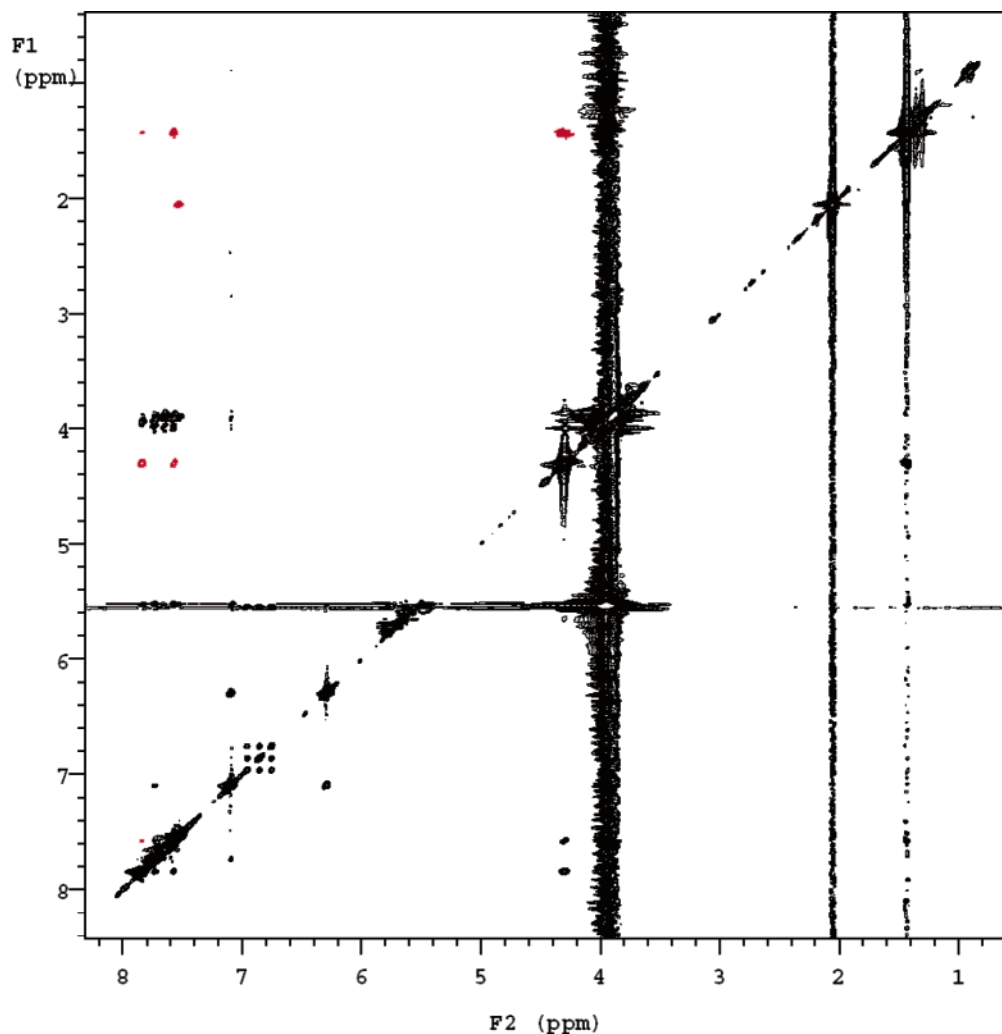


Figure 7. 2D ROESY (100 ms) spectrum of AcGGAGGNH₂ dissolved in TFE. Protons used in the conformational analysis of the Ala3 structure are assigned as Acetyl H β (2.06 ppm), Gly1 HN (7.54 ppm), Ala3 H α (4.30 ppm), Ala3 H β (1.43 ppm), Ala3 HN (7.57 ppm), and Gly4 HN (7.84 ppm). The ROE cross-peaks colored in red are the ones integrated to derive distances.

spectrum obtained by subtracting the spectrum of G₂AG₂ at 20% TFE from that at 80% indeed shows that conformers other than PII are favorable in high TFE concentration (inset, Figure 3b).

Denaturing cosolvents such as GuHCl have been reported to favor PII in proline-containing peptides, on the other hand.⁷³ Figure 5 shows the effect of different concentrations of GuHCl on the CD spectrum of O₂A₇O₂. As in Pro-rich peptide models, the CD spectrum shows increasing PII content as the GuHCl concentration increases. We could not detect a comparable effect in G₂AG₂, and this sensitivity might reflect ionic effects on the flanking bases as well. Agents such as SDS that normally favor helix formation stabilize α -helix in O₂A₇O₂, shown in Figure 6, but show a much smaller effect on G₂AG₂, as shown in Figure 3c.

Structure Calculations of G₂AG₂ in TFE. A total of 15 ROESY peaks were identified in the ¹H spectrum of G₂AG₂. The conformation of the residues Ala3, Gly4, and Gly5 is most restricted because 12 ROEs are observed for the last three residues of the peptide. The ROEs colored red in the spectrum shown in Figure 7 were used to carry out a structural analysis of Ala3.

Table 1. ROE Distances Used for the Structure Calculation of AcGGAGGNH₂ in TFE

assignment	ROE volume	calculation volume	fixed distance (Å)	calculated distance (Å)
AcHb–Gly1HN	-5.84×10^7	-1.95×10^7	2.96	
Ala3Hb–Ala3Ha	-9.64×10^7	-3.21×10^7	2.54	
Ala3Ha–Ala3HN	-2.01×10^7	-2.01×10^7		2.94
Ala3Ha–Gly4HN	-8.21×10^7	-8.21×10^7		2.33
Ala3Hb–Ala3HN	-9.47×10^7	-3.16×10^7		2.73
Ala3Hb–Gly4HN	-5.63×10^6	-1.88×10^6		4.37
Ala3HN–Gly4HN	-5.54×10^6	-5.54×10^6		3.91

We employed a pseudo-atom to represent the methyl protons. The original ROE volumes were divided by 3 in the case of methyl protons. Coordinates for the peptide G₂AG₂ were built using the Biopolymer module of Insight II. The ROE distances were calibrated using two fixed references. One is the distance between the α protons of the N-terminal acetyl group and the amide proton of Gly1. The second is the distance between α and β protons of Ala3. The ROE coefficients *Acn* and *Acc* were calculated from these two distances as $Acn = -1.31 \times 10^{+10}$, $Acc = -8.63 \times 10^{+09}$, so that $Ann = Acn^2/Acc = -1.99 \times 10^{+10}$.

These three coefficients were used to calculate the distances in Table 1.

(73) Tiffany, M. L.; Krimm, S. *Biopolymers* **1973**, *12*, 575–587.

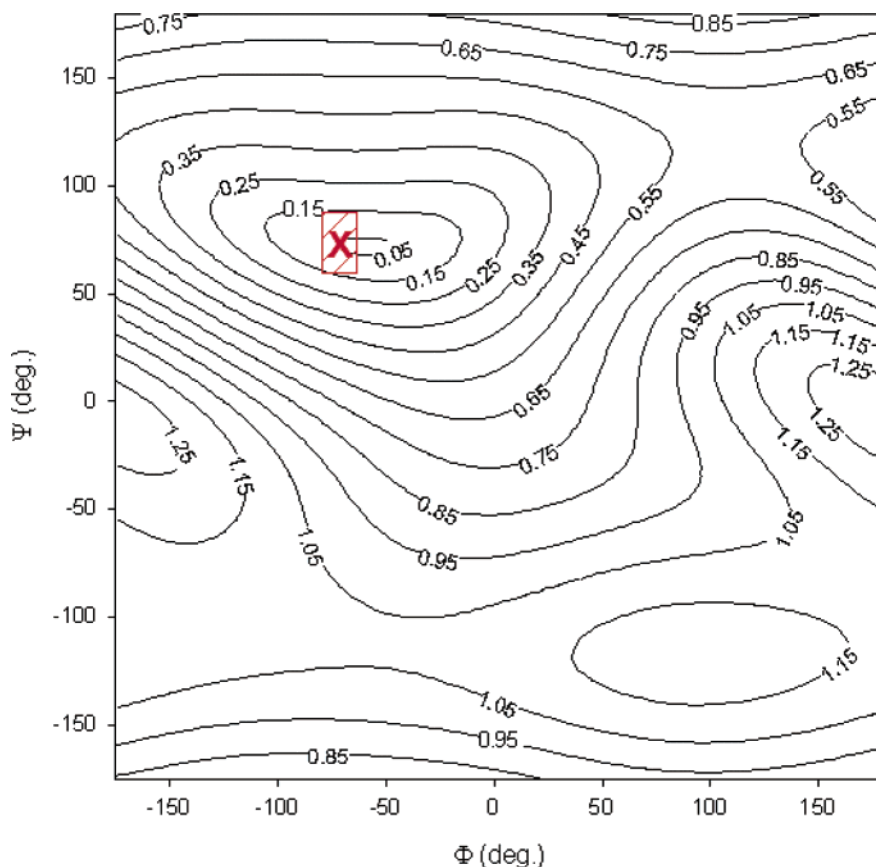


Figure 8. 3D contour of root-mean-square distance errors versus ϕ and ψ dihedral angles of Ala3 in AcGGAGGNH₂. The reasonable conformation ensemble is in a 0.15 Å well. The structure is further restricted into a red crosshatched region when the ϕ angle is restricted by the $^3J_{\alpha N}$ coupling constant.

The dihedral angles ϕ and ψ of Ala3 were varied independently at 5° intervals. The ROE distances in Table 1 were calculated for each of 5184 (72 × 72) conformations. The set of root-mean-square distance error (rmsde) contours was then overlaid on a Ramachandran plot, as shown in Figure 8.

ROE volumes were estimated from Gaussian integration using SPARKY. All integrations show an error below 10%, which corresponds to a maximum ROE distance error of 0.14 Å (calculation not shown). The most probable structure defined by this plot corresponds to the “valley” region in which the conformations all have an rmsd value below 0.15 Å with $\phi = -63^\circ \pm 40^\circ$ and $\psi = 72^\circ \pm 17^\circ$.⁴¹

The measured value of the $^3J_{\alpha N}$ coupling constant, 5.1 ± 1 Hz, restricts the ϕ angle to between -80° and -65° . This further confines the Ala3 structure to the region designated by the red cross in Figure 8, corresponding to $\phi = -75^\circ \pm 10^\circ$ and $\psi = 72^\circ \pm 15^\circ$. While our data are insufficient to define the structure around the central Ala more precisely, the effect of these constraints is to make the presence of substantial β structure highly unlikely. The structure adopted by Ala3 in TFE is most consistent with a γ turn ($\phi = -78^\circ$, $\psi = 65^\circ$). Assigning a unique conformation to the ensemble of conformations in any short peptide such as G₂AG₂ is risky. This conclusion is based on use of experimental distances exclusively without any energy minimization. The root-mean-square error of distances involved in the calculation is only 0.15 Å, indicating that the ROE volumes are accurate and therefore that the γ turn structural assignment may be appropriate. An intramolecular hydrogen bond between the carbonyl oxygen of Gly2 and the amide hydrogen of Gly4 is also observed. This is missing in the

conformation of G₂AG₂ dissolved in H₂O. On the other hand, we reiterate that calculated CD spectra of the peptide appear to be more consistent with a mixture of conformations rather than any single dominant turn structure. It is conceivable that due to the large difference in the time scales of their conformational averaging the CD and NMR report different averages. The firm conclusion is that internally H-bonded turn conformations predominate in TFE, in contrast to the PII structure evident in water.

Discussion

These results extend previous studies on di- and trialanine peptides and similar models, which show that PII is an important component of the structure in water and is highly sensitive to effects of solvation.²¹ What we find that is new is that in a neutral fragment with minimal steric constraints, modeled by G₂AG₂, the PII structure adopted by Ala in water is destabilized by solvents such as simple alcohols linearly according to empirical scales of overall polarity rather than dielectric constant, for example, or any other single solvent property. This is consistent with the hypothesis that water molecules participate in maintaining the PII conformation. In vacuo, many calculations indicate that a γ turn is the state of lowest energy.⁷⁴ In water, PII is favored over β , because of either favorable H-bonding with water molecules or minimal perturbation of water–water interactions.^{75,76}

(74) Hu, H.; Elstner, M.; Hermans, J. *Proteins: Struct., Funct., Genet.* **2003**, *50*, 451–463.

(75) Drozdov, A. N.; Grossfield, A.; Pappu, R. V. *J. Am. Chem. Soc.* **2004**, *126*, 2574–2581.

If dominated by one conformation, the structure of G₂AG₂ in neat TFE that we define is close to γ turn, as inferred from the NMR constraint analysis. As expected in the longer O₂A₇O₂ peptide with 7 adjacent alanines, the structure in TFE is α helical, consistent with a wealth of evidence that TFE promotes helical structure.^{71,77–80} This effect has been attributed to the fact that TFE enhances internal H-bonds in native helical structure, based on measuring the shift in pK_a of an internally H-bonded small molecule as reference.^{78,79} An alternative interpretation has been presented, that TFE acts by disrupting solvent structure(s) that stabilize unfolded conformations.⁸⁰ Our results here suggest that the two views may not in fact be distinguishable: TFE destabilizes PII conformation and concomitantly populates internally H-bonded alternative structures, γ turn in short chains and α helix in chains long enough to nucleate this helix. Interestingly, the detergent SDS stabilizes α -helical structure in O₂A₇O₂, while it has little effect on G₂AG₂ at similar concentrations. This may be due to the affinity of SDS for the positive charges in the former. Thus, the difference in CD spectra seen in Figure 6 and Figure 3c may reflect the

association of the neutralized peptide rather than intrinsically higher monomeric helicity. The classical protein denaturing cosolvent GuHCl has no observable effect on the PII conformation of G₂AG₂, which is consistent with earlier NMR results on G₂XG₂.⁸¹ The fact that the PII conformation in O₂A₇O₂ can be stabilized by addition of GuHCl indicates that conformations other than PII can convert to PII. This is consistent with the idea that the completely unfolded state of peptide in water is PII at low temperature. The process of helix formation in water has been investigated recently by simulations as well as in experiments.^{36,82} Simulations using bulk solvent parameters as well as explicit water molecules reveal PII structure in water. In particular, Garcia detects specific hydration patterns corresponding to PII structure.

Acknowledgment. This work was supported by a grant from ONR to N.R.K. and NIH research grant EB02803 (formerly GM22994) to R.W.W. We thank Angel Garcia, Tobin Sosnick, and Alex Kentsis for helpful discussions. We thank Dr. Yun Xiang for writing Fortran code for bond rotations.

JA047594G

(76) Mezei, M.; Fleming, P. J.; Srinivasan, R.; Rose, G. D. *Proteins* **2004**, *55*, 502–507.

(77) Nelson, J. W.; Kallenbach, N. R. *Proteins* **1986**, *1*, 211–217.

(78) Luo, P.; Baldwin, R. L. *Biochemistry* **1997**, *36*, 8413–8421.

(79) Luo, P.; Baldwin, R. L. *J. Mol. Biol.* **1998**, *279*, 49–57.

(80) Kentsis, A.; Sosnick, T. R. *Biochemistry* **1998**, *37*, 14613–14622.

(81) Plaxco, K. W.; Morton, C. J.; Grimshaw, S. B.; Jones, J. A.; Pitkeathly, M.; Campbell, I. D.; Dobson, C. M. *J. Biomol. NMR* **1997**, *10*, 221–230.

(82) Garcia, A. E.; Onuchic, J. N. *Proc. Natl. Acad. Sci. U.S.A.* **2003**, *100*, 13898–13903.